



## Hydroelastic behaviour of compound floating plate in waves

T.I. KHABAKHPASHEVA and A.A. KOROBKIN

*Lavrentyev Institute of Hydrodynamics, Siberian Division of Russian Academy of Sciences, Lavrentyev Prospect 15, Novosibirsk, 630090, Russia (e-mail: tana@hydro.nsc.ru, kaa@hydro.nsc.ru)*

Received 26 June 2001; accepted in revised form 14 February 2002

**Abstract.** The paper deals with the plane problem of the hydroelastic behaviour of floating plates under the influence of periodic surface water waves. Analysis of this problem is based on hydroelasticity, in which the coupled hydrodynamics and structural dynamics problems are solved simultaneously. The plate is modeled by an Euler beam. The method of numerical solution of the floating-beam problem is based on expansions of the hydrodynamic pressure and the beam deflection with respect to different basic functions. This makes it possible to simplify the treatment of the hydrodynamic part of the problem and at the same time to satisfy accurately the beam boundary conditions. Two approaches aimed to reduce the beam vibrations are described. In the first approach, an auxiliary floating plate is added to the main structure. The size of the auxiliary plate and its elastic characteristics can be chosen in such a way that deflections of the main structure for a given frequency of incident wave are reduced. Within the second approach the floating beam is connected to the sea bottom with a spring, the rigidity of which can be selected in such a way that deflections in the main part of the floating beam are very small. The effect of the vibration reduction is quite pronounced and can be utilized at the design stage.

**Key words:** bending moments, deflection, floating plate, hydroelasticity, incident wave, pre-cracked plate.

### 1. Introduction

Very large floating structures are considered as an alternative of such land-based large facilities as, for example, airports (Suzuki and Yoshida [1]). A proposed design of a floating airport has a thin-plate configuration of large horizontal extent. The bending rigidity of such a floating plate is small, and wave-induced motion of the plate is significantly affected by its elastic deflection. The analysis of floating-plate behaviour in waves is based on hydroelasticity, in which the coupled hydrodynamics and structural dynamics problems are solved simultaneously. A goal of the analysis is to predict accurately both the plate deflection and stresses in the plate and to find ways to reduce these. The latter is of great importance for securing safety and the structure's performance. Reduction of the motion of a floating elastic plate in waves by surrounding it by a breakwater was studied numerically by Nagata *et al.* [2] and by Seto and Ochi [3]. It was shown that breakwaters effectively reduce plate response for long waves but in the case of short waves the reduction is not large. The idea to put a floating structure in the shadow of a breakwater for reduction of the structure response is clear and practical. However, the problem in this case is that the environment in the ocean may be affected adversely by the construction of bottom-mounted breakwaters. Another way to reduce the floating-plate response was suggested by Yago *et al.* [4], which is to adjust a wave reflector to the front side of the elastic plate. This is a vertical submerged plate, the height of which is about three times less than the water depth, or a wave-breaking structure which is a multi-column floating structure of smaller extent. Experiments revealed that both the wave reflector and the wave-breaking structure decrease deflections of the main structure in the case

of short incident waves. However, for long incident waves which provide greater deflections of the main structure than short waves, the experiments did not detect sizeable effects of the additional structures. Both approaches by Seto and Ochi [3] and by Yago *et al.* [4] are based on the idea to protect (to shield) a floating elastic structure from the incident wave action, in order to reduce a part of the wave energy which can be absorbed by the structure.

In order to test possible approaches aimed to reduce floating-plate response in waves, direct numerical simulations of hydroelastic behaviour of the plate are very attractive. Three-dimensional numerical simulation of the linear response of an elastic plate in waves is the most accurate approach accurate approach at the present time. Three-dimensional numerical simulations of floating rectangular plates in waves were performed by Kashiwagi [5] and by Kim and Ertekin [6] among others. However, these simulations are still time-consuming and expensive to use at the design stage. At the very initial stage of design it looks reasonable to use the simplest models of floating-plate behaviour, in order to discover main trends and to distinguish main features of the problem. If an effect is well-pronounced within a simple model, it is expected to be of importance also within more accurate models. In this paper two approaches to reduce elastic deflection of floating plates are described within the framework of a two-dimensional linear theory. The plate is modeled by an Euler Beam.

The first approach is based on the concept of a vibration absorber which is well-known in many engineering application such as rotation machinery (see, for example, Shabana [7, Chapter 6], where single-degree-of-freedom systems are used. A traditional way of avoiding undesirable vibration conditions is to change the system stiffness and its inertia characteristics. On the other hand, it is possible to convert a single-degree-of-freedom system to a two-degree-of-freedom mechanical system by adding an auxiliary spring-and-mass system. The parameters of the added system can be selected in such a way that the vibration of the main system is essentially reduced. The case of a floating elastic plate is more complicated than that of a single-degree-of-freedom system. Nevertheless, the idea of a vibration absorber is also helpful for the design of large floating structures. The idea is to add to the main floating structure an auxiliary floating plate of smaller size, with its own stiffness and inertia characteristics, and to select the size of the auxiliary plate and its characteristics, which provide reduction of the main structure deflections for a given frequency of the incident wave. The auxiliary plate can be adjacent, either in front of the main plate or at its rear side. Even within the two-dimensional linear theory the hydroelastic problem of floating plate is very complicated, which is why we do not expect that simple formulae for the optimal parameters of the auxiliary plate can be obtained. Numerical calculations have been performed to demonstrate the effect of reduction of the main plate deflection with the help of an auxiliary adjacent floating plate. A more rational way to obtain the characteristics of the auxiliary plate is not obvious at this moment.

Within the second approach the floating beam is connected to the sea bottom with a spring, the rigidity of which can be adjusted in such a way that the beam deflection due to incident waves is reduced.

Both approaches lead to coupled problems in hydroelasticity, which are treated by the common method described in the present paper. The developed method is applied to the problem of a homogeneous free-free floating plate in waves, for which experimental data are available. The method is also applied to problem of a pre-cracked floating plate.

The formulation of the problem is given in Section 2. The method of analysis is described in Section 3. Four cases are studied numerically, namely the floating beam is:

- (i) homogeneous and free-free (Section 4),

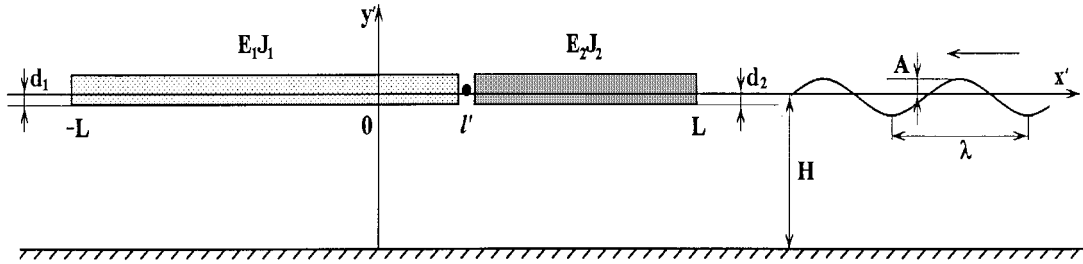


Figure 1. Basic configuration and notations.

- (ii) pre-cracked and free-free (Section 5),
- (iii) compound with an elastic connection between the parts of the beam (Section 6),
- (iv) homogeneous and elastically connected to the sea bottom (Section 7).

The formulation is given for the third problem on compound beam behaviour.

## 2. Formulation of the problem

The hydroelastic behaviour of two connected floating beams in waves is considered by means of a linear two-dimensional theory (see Figure 1). The beams are of constant thickness and homogeneous. They are connected with a torsional spring of stiffness  $K_T$ . The drafts of the beams,  $d_1$  and  $d_2$ , are assumed to be much smaller than both the total beam length  $2L$  and the liquid depth  $H$ . The bending stiffnesses  $E_1J_1$  and  $E_2J_2$  of the beams and their drafts  $d_1$  and  $d_2$ , are given. The beam vibrations are caused by a periodic incident wave of frequency  $\omega$  and small amplitude  $A$ . The longer beam is referred to as the main structure, the elastic characteristics of which are prescribed. The shorter beam is referred to as the auxiliary plate, the length of which is given. The midpoint of the whole structure is taken as the origin of the Cartesian coordinate system  $x'Oy'$  (dimensional variables are denoted by a prime). The right-hand-side plate (see Figure 1) is treated as the auxiliary one if  $l' > 0$  and as the main structure if  $l' < 0$ . The flow region,  $-H < y' < 0$ , is bounded from below by a horizontal undeformable bottom,  $y' = -H$ . The part of the upper boundary  $-L < x' < L$ ,  $y' = 0$  corresponds to the floating structure, and the parts  $x' < -L$  and  $x' > L$  correspond to the free surface. The liquid is assumed to be ideal and incompressible, and its flow two dimensional and potential. Within the framework of a linear theory the liquid flow is described by the velocity potential  $\phi'(x', y', t')$ , and the structure's vibration by its normal deflection  $w'(x', t')$ , where  $t'$  is time. The beam deflection  $w'(x', t')$  is governed by the Euler equation, whose constant coefficients are different for the main structure and for the auxiliary plate. We shall determine the beam deflection and the stress distribution in the beams and study their dependence on the characteristics of the beam parts and conditions of their connection. In particular, we need to determine both the characteristics of the auxiliary plate and the torsional spring stiffness  $K_T$ , which essentially reduce the vibration amplitude of the main plate.

Non-dimensional variables are used below. The half-length of the whole structure  $L$  is taken as the length scale;  $1/\omega$  as the time scale, where  $\omega$  is the incident-wave frequency; the amplitude of the incident wave  $A$  as the deflection scale; the product  $\rho g A$ , where  $\rho$  is the liquid density and  $g$  is the acceleration due to gravity, as the pressure scale;  $2L_m d_m A \rho g$  as the scale of the bending moments, where  $d_m$  is the draft and  $L_m$  is the length of the main structure ( $d_m = d_1$ ,  $L_m = (L + l')/2$  if  $l' > 0$  and  $d_m = d_2$ ,  $L_m = (L - l')/2$  if  $l' < 0$ ); and the product

$A\omega L$  as the scale of the velocity potential. It should be noted that the frequency of the incident wave is equal to unity and the total structure length to 2 in non-dimensional variables.

Within the linear theory the velocity potential of the flow  $\phi(x, y, t)$  satisfies the following equations

$$\begin{aligned} \phi_{xx} + \phi_{yy} &= 0, \quad (-\infty < x < +\infty, -H_0 < y < 0), \\ \phi_y &= 0, \quad (y = -H_0), \\ \phi_y &= \eta_t, \quad \gamma\phi_t + \eta = 0, \quad (y = 0, \quad |x| > 1), \\ \phi_y &= w_t(x, t), \quad (y = 0, \quad |x| < 1), \end{aligned} \quad (1)$$

where  $H_0 = H/L$ ,  $\gamma = L\omega^2/g$ ; the equation  $y = \eta(x, t)$  describes the free surface shape. In non-dimensional variables the deflection  $w(x, t)$  of the structure is governed by the Euler beam equation

$$\alpha(x)w_{tt} + \beta(x)w_{xxxx} = p(x, 0, t), \quad (|x| < 1) \quad (2)$$

and the boundary conditions

$$\begin{aligned} w_{xx}(\pm 1, t) &= 0, \quad w_{xxx}(\pm 1, t) = 0, \\ w(l-0, t) &= w(l+0, t), \end{aligned} \quad (3)$$

$$\begin{aligned} \beta_1 w_{xx}(l-0, t) &= \beta_2 w_{xx}(l+0, t), \\ \beta_1 w_{xxx}(l-0, t) &= \beta_2 w_{xxx}(l+0, t) \end{aligned} \quad (4)$$

$$w_{xxl}(l-0, t) + k_T[w_x(l-0, t) - w_x(l+0, t)] = 0, \quad (5)$$

where  $d_j = d_1$ ,  $\alpha(x) = \alpha_1$  and  $\beta(x) = \beta_1$  when  $-1 < x < l$ ;  $d_j = d_2$ ,  $\alpha(x) = \alpha_2$  and  $\beta(x) = \beta_2$  when  $l < x < 1$ ,  $l = l'/L$ ;  $\alpha_j = \gamma d_j/L$ ,  $\beta_j = E_j J_j/(\rho g L^4)$ , ( $j = 1, 2$ );  $k_T = K_T L/E_1 J_1$  is the dimensionless local flexibility coefficient.

The hydrodynamic pressure on the structure is given by the equation

$$p(x, t) = -\gamma\phi_t(x, 0, t) - w(x, t),$$

and the bending-moment distribution by

$$M(x, t) = -\beta(x)L^2/(2a_m d_m)w_{xx}(x, t),$$

where  $a_m = 1 + l$ ,  $d_m = d_1$  if  $l > 0$  and  $a_m = 1 - l$ ,  $d_m = d_2$  if  $l < 0$ . It should be noted that the longer part of the beam is referred to as the main structure and the scaling of the bending moments corresponds to this part.

We seek a solution of problem (1–5) subject to the following conditions on the behavior of the free surface as  $x \rightarrow \pm\infty$ :

$$\begin{aligned} \eta(x, t) &\sim \cos(kx + t) + A^{(+)} \cos(kx - t + \delta^{(+)}) \quad (x \rightarrow +\infty), \\ \eta(x, t) &\sim A^{(-)} \cos(kx + t + \delta^{(-)}) \quad (x \rightarrow -\infty), \end{aligned} \quad (6)$$

where  $A^{(+)}$  and  $A^{(-)}$  are the amplitudes of the reflected and transmitted waves divided by the amplitude of the incident wave,  $\delta^{(+)}$  and  $\delta^{(-)}$  are the corresponding phase shifts, and  $k$  is a dimensionless wavenumber that is a positive solution of the equation  $k \tanh kH_0 =$

$\gamma$ . The wavelength of the incident wave  $\lambda$  in dimensional variables is given by the formula  $\lambda = 2\pi L/k$ . The quantities  $A^{(+)}$ ,  $A^{(-)}$ ,  $\delta^{(+)}$  and  $\delta^{(-)}$  are unknown beforehand and must be determined, together with the flow parameters and the plate deflection  $w(x, t)$ .

It should be noted that initial data are absent in the formulation of the problem (1–6), which is due to the assumption that at large times the flow is time-periodic and independent of the distinctive features of the initial conditions. The velocity potential  $\phi(x, y, t)$  of the developed wave motion of the fluid, the beam deflection  $w(x, t)$  and the pressure  $p(x, y, t)$  are sought in the forms

$$\phi(x, y, t) = \phi_i(x, y, t) + \Re\{i \exp(it)\Phi(x, y)\}, \quad w(x, t) = \Re\{\exp(it)W(x)\}, \quad (7)$$

$$p(x, 0, t) = \Re\{\exp(it)P(x)\}, \quad \phi_i(x, y, t) = -\frac{1}{\gamma} \frac{\cosh[k(y + H_0)]}{\cosh(kH_0)} \sin(kx + t), \quad (8)$$

where  $\phi_i(x, y, t)$  is the velocity potential of the incident wave in the absence of the floating plate. The new unknown functions  $\Phi(x, y)$ ,  $W(x)$ , and  $P(x)$  are complex-valued. Substituting (7) and (8) in (1–5), we obtain

$$\Phi_{xx} + \Phi_{yy} = 0, \quad (-\infty < x < +\infty, \quad -H_0 < y < 0), \quad (9)$$

$$\Phi_y = 0, \quad (y = -H_0), \quad (10)$$

$$\Phi_y = \gamma\Phi, \quad (y = 0, \quad |x| > 1), \quad (11)$$

$$\Phi_y = W(x) - \exp(ikx), \quad (y = 0, \quad |x| < 1), \quad (12)$$

$$P(x) = \gamma\Phi(x, 0) - W(x) + \exp(ikx), \quad (|x| < 1), \quad (13)$$

$$\beta(x)W^{IV} - \alpha(x)W = P(x), \quad (|x| < 1), \quad (14)$$

$$W''(\pm 1) = 0, \quad W'''(\pm 1) = 0, \quad (15)$$

$$W(l-0) = W(l+0), \quad \beta_1 W''(l-0) = \beta_2 W''(l+0), \quad \beta_1 W'''(l-0) = \beta_2 W'''(l+0), \quad (16)$$

$$W''(l-0) + k_T[W'(l-0) - W'(l+0)] = 0. \quad (17)$$

In terms of the new variables the radiation conditions (6) have the forms

$$\Phi(x, 0) \sim B^{(+)} \exp(-ikx), \quad (x \rightarrow +\infty), \quad \Phi(x, 0) \sim B^{(-)} \exp(ikx), \quad (x \rightarrow -\infty), \quad (18)$$

where the coefficients  $B^{(+)}$  and  $B^{(-)}$  have to be determined, together with the solution of the boundary-value problem (9–17),  $A^{(+)} = \gamma|B^{(+)}|$ ,  $\delta^{(+)} = -\arg B^{(+)}$  and  $A^{(-)} = |1 + \gamma B^{(-)}|$ ,  $\delta^{(-)} = \arg(1 + \gamma B^{(-)})$ .

Equations (9–12) and (18) represent the hydrodynamic part of the coupled problem. This part can be reduced to the integral equation for the hydrodynamic pressure  $P(x)$  along the plate

$$P(x) + \frac{\gamma}{2\pi} \int_{-1}^1 P(x_0)K(x-x_0) dx_0 = e^{ikx} - W(x). \quad (19)$$

The function  $K(z)$  in (19) is given as

$$K(z) = -2\pi i \frac{ke^{-ik|z|}}{H_0(k^2 - \gamma^2) + \gamma} + 2\pi \sum_{j=1}^{\infty} \frac{s_j e^{-s_j|z|}}{H_0(s_j^2 + \gamma^2) - \gamma},$$

where  $s_j = (\pi j - d_j)/H_0$  and  $\delta_j$  is the solution of the equation  $\delta_j = \arctan(\gamma H_0/(\pi j - \delta_j))$ ,  $j \geq 1$ .

To derive the integral equation (19), we have assumed that the pressure  $P(x)$  is known along the plate. Then the boundary-value problem defined by (9–11) and (18) together with the condition  $\gamma\Phi - \Phi = P(x)$ , where  $y = 0$ ,  $|x| < 1$ , is solved with the help of the Fourier transform. The resulting solution gives the potential  $\Phi(x, 0)$  along the plate as a convolution integral. Substituting this integral in Equation (13), we arrive finally at Equation (19).

Below we solve the problem (14), (19) with the boundary conditions (15)–(17) numerically. We shall determine the amplitude of the plate deflection  $|W(x)|$  and that of the bending moments  $|M(x)| = \max_t |M(x, t)|$  for given characteristics of the incident wave and the beam.

### 3. Method of solution

Problem (14), (19) can be solved with the help of the normal-mode method in the same manner as in [8] with eigenfunctions of the compound beam as basic functions. This method reduces the integral equation (19) to an infinite system of algebraic equations with respect to the principle coordinates of the pressure  $P(x)$ . However, the eigenfunctions of the compound beam are rather complicated and, moreover, they do not correspond to the features of the pressure distribution along the beam. A main idea of the present study is to use different basic functions for the pressure and the beam deflection. Trigonometric functions are used as basic ones to present the pressure in the form

$$P(x) = \frac{1}{2}a_0 + \sum_{n=1}^{\infty} a_n^{(c)} \cos \pi n x + \sum_{n=1}^{\infty} a_n^{(s)} \sin \pi n x. \quad (20)$$

Substitution of expansion (20) in equation (14) leads to the following expansion for the beam deflection

$$W(x) = \frac{1}{2}a_0 w_0^{(c)}(x) + \sum_{n=1}^{\infty} a_n^{(c)} w_n^{(c)}(x) + \sum_{n=1}^{\infty} a_n^{(s)} w_n^{(s)}(x). \quad (21)$$

The functions  $w_n^{(c)}(x)$  and  $w_n^{(s)}(x)$  satisfy conditions (15–17) and Equation (14) with  $P(x)$  being replaced by  $\cos(n\pi x)$  and  $\sin(n\pi x)$ , respectively. The functions  $w_n^{(c)}(x)$  and  $w_n^{(s)}(x)$  are considered here as basic functions for the beam deflection.

The integral equation (19) accounting for expansions (20) and (21) leads to an infinite system of algebraic equations with respect to the coefficients  $a_{c_n}$  and  $a_{s_n}$ . If  $N$  terms in each sum of the expansions (20) and (21) are taken into account, then the system can be presented in matrix form as follows:

$$\left( \mathbf{I} + \frac{\gamma}{2\pi} \mathbf{S} + \mathbf{A} \right) \vec{a} = \vec{e}, \quad (22)$$

where  $\mathbf{I} = \text{diag}(2, 1, 1, \dots)$  is the diagonal matrix; the symmetric matrix  $\mathbf{S}$  comes from the integral term in (19) and the symmetric matrix  $\mathbf{A}$  comes from the term  $W(x)$ , and  $\vec{a} =$

$(a_0/2, a_1^{(c)}, a_2^{(c)}, \dots, a_N^{(c)}, a_1^{(s)}, a_2^{(s)}, \dots, a_N^{(s)})^T$ . The elements of the vector  $\vec{e}$  are the coefficients in the expansion of  $\exp(ikx)$  with respect to the trigonometric functions. The sizes of the matrices  $\mathbf{I}$ ,  $\mathbf{S}$  and  $\mathbf{A}$  in Equation (22) are equal to  $(2N + 1) \times (2N + 1)$ . The matrix  $\mathbf{S}$  has the form

$$\mathbf{S} = \left( \begin{array}{cccc|cccc}
 S_{00}^{cc} & S_{01}^{cc} & S_{02}^{cc} & \cdots & S_{0N}^{cc} & S_{01}^{sc} & S_{02}^{sc} & \cdots & S_{0N}^{sc} \\
 S_{10}^{cc} & S_{11}^{cc} & S_{22}^{cc} & \cdots & S_{2N}^{cc} & S_{11}^{sc} & S_{12}^{sc} & \cdots & S_{1N}^{sc} \\
 S_{20}^{cc} & S_{21}^{cc} & S_{22}^{cc} & \cdots & S_{2N}^{cc} & S_{21}^{sc} & S_{22}^{sc} & \cdots & S_{2N}^{sc} \\
 \cdot & \cdot & \cdot & \cdots & \cdot & \cdot & \cdot & \cdots & \cdot \\
 S_{N0}^{cc} & S_{N1}^{cc} & S_{N2}^{cc} & \cdots & S_{NN}^{cc} & S_{N1}^{sc} & S_{N2}^{sc} & \cdots & S_{NN}^{sc} \\
 \hline
 S_{10}^{sc} & S_{11}^{sc} & S_{12}^{sc} & \cdots & S_{1N}^{sc} & S_{11}^{ss} & S_{12}^{ss} & \cdots & S_{1N}^{ss} \\
 S_{20}^{sc} & S_{21}^{sc} & S_{22}^{sc} & \cdots & S_{2N}^{sc} & S_{21}^{ss} & S_{22}^{ss} & \cdots & S_{2N}^{ss} \\
 \cdot & \cdot & \cdot & \cdots & \cdot & \cdot & \cdot & \cdots & \cdot \\
 S_{N0}^{sc} & S_{N1}^{sc} & S_{N2}^{sc} & \cdots & S_{NN}^{sc} & S_{N1}^{ss} & S_{N2}^{ss} & \cdots & S_{NN}^{ss}
 \end{array} \right),$$

where

$$S_{nm}^{cc} = \int_{-1}^1 \int_{-1}^1 K(x-y) \cos(\pi nx) \cos(\pi my) dx dy, \quad (n \geq 0, m \geq 0),$$

$$S_{nm}^{sc} = \int_{-1}^1 \int_{-1}^1 K(x-y) \sin(\pi nx) \cos(\pi my) dx dy, \quad (n > 0, m \geq 0),$$

$$S_{nm}^{ss} = \int_{-1}^1 \int_{-1}^1 K(x-y) \sin(\pi nx) \sin(\pi my) dx dy, \quad (n > 0, m > 0).$$

It is clear that the matrix  $\mathbf{S}$  is symmetric. Moreover,  $S_{nm}^{sc} = 0$  ( $n = 0, 1, 2, \dots, m = 1, 2, 3, \dots$ ), which follows from the equality  $K(-z) = K(z)$ . It can be shown that the matrix  $\mathbf{A}$  is also symmetric and has a form similar to that of matrix  $\mathbf{S}$ . Once the functions  $w_n^{(c)}(x)$  and  $w_n^{(s)}(x)$  have been determined, we obtain

$$A_{nm}^{cc} = \int_{-1}^1 w_n^{(c)}(x) \cos(\pi mx) dx, \quad (n \geq 0, m \geq 0); \quad (23)$$

$$A_{nm}^{sc} = \int_{-1}^1 w_n^{(s)}(x) \cos(\pi mx) dx = \int_{-1}^1 w_m^{(c)}(x) \sin(\pi nx) dx, \quad (n > 0, m > 0); \quad (24)$$

$$A_{nm}^{ss} = \int_{-1}^1 w_n^{(s)}(x) \sin(\pi mx) dx, \quad (n > 0, m > 0). \quad (25)$$

The elements of the matrices  $\mathbf{S}$  and  $\mathbf{A}$  and those of the vector  $\vec{e}$  are given by analytical formulae, which are not reproduced here. The matrix  $\mathbf{A}$  is different for each of the problems listed in Section 1. Other elements of the algebraic system (22) are common for each particular problem.

#### 4. Free-free homogeneous beam

The problem under consideration with  $\alpha_1 = \alpha_2$ ,  $\beta_1 = \beta_2$  and  $k_T = \infty$  corresponds to that of hydroelastic behaviour of the homogeneous free-free beam in waves. In this case the basic functions  $w_n^{(c)}(x)$ , ( $n \geq 0$ ) satisfy the following equations

$$\beta \frac{d^4 w_n^{(c)}}{dx^4} - \alpha w_n^{(c)} = \cos(\pi n x) \quad (|x| < 1); \quad (26)$$

$$\frac{d^2 w_n^{(c)}}{dx^2}(\pm 1) = 0, \quad \frac{d^3 w_n^{(c)}}{dx^3}(\pm 1) = 0. \quad (27)$$

The functions  $w_n^{(s)}(x)$  ( $n > 0$ ) are determined as solutions of the boundary-value problem (26)–(27) with  $\cos(\pi n x)$  being replaced by  $\sin(\pi n x)$ . Exact solutions of these problems are given by the formulae:

$$w_0^{(c)}(x) = -1/\alpha, \quad w_n^{(c)}(x) = \frac{\cos \pi n x}{\beta(\pi n)^4 - \alpha} + \frac{(-1)^n (\pi n)^2 (\cosh \lambda x \sin \lambda - \cos \lambda x \sinh \lambda)}{\lambda^2 (\beta(\pi n)^4 - \alpha) [\cos \lambda \sinh \lambda + \cosh \lambda \sin \lambda]}, \quad (28)$$

$$w_n^{(s)}(x) = \frac{\sin \pi n x}{\beta(\pi n)^4 - \alpha} + \frac{(-1)^n (\pi n)^3 (\sin \lambda x \sinh \lambda + \sinh \lambda x \sin \lambda)}{\lambda^2 (\beta(\pi n)^4 - \alpha) [\cosh \lambda \sin \lambda - \cos \lambda \sinh \lambda]}, \quad (29)$$

where  $\lambda = \sqrt[4]{\alpha/\beta}$ . Substituting (28)–(29) in (23)–(25), we find the elements of matrix  $\mathbf{A}$

$$A_{nm}^{cc} = A_{mn}^{cc} = \frac{\delta_{nm}}{(\beta\pi^4 n^4 - \alpha)} + \frac{4\pi^2 n^2 m^2 (-1)^{n-m} \beta}{\lambda (\cot \lambda + \coth \lambda) (\beta\pi^4 n^4 - \alpha) (\beta\pi^4 m^4 - \alpha)},$$

$$A_{nm}^{ss} = A_{mn}^{ss} = \frac{\delta_{nm}}{(\beta\pi^4 n^4 - \alpha)} - \frac{4\pi^6 n^3 m^3 (-1)^{n-m} \beta}{\lambda^3 (\coth \lambda - \cot \lambda) (\beta\pi^4 n^4 - \alpha) (\beta\pi^4 m^4 - \alpha)},$$

$$A_{00}^{cc} = -2/\alpha, \quad A_{n0}^{cs} = A_{0n}^{sc} = 0, \quad A_{n0}^{cc} = A_{0n}^{cc} = 0, \quad A_{nm}^{sc} = A_{nm}^{cs} = 0 \quad (n, m > 0).$$

Here  $\delta_{nm} = 0$  if  $m \neq n$  and  $\delta_{nn} = 1$  if  $m = n$ . As a result, the matrix  $\mathbf{A}$  has the form

$$\mathbf{A} = \begin{pmatrix} A_{00}^{cc} & 0 & 0 & \dots & 0 & 0 & 0 & \dots & 0 \\ 0 & A_{11}^{cc} & A_{12}^{cc} & \dots & A_{1N}^{cc} & 0 & 0 & \dots & 0 \\ 0 & A_{21}^{cc} & A_{22}^{cc} & \dots & A_{2N}^{cc} & 0 & 0 & \dots & 0 \\ \cdot & \cdot & \cdot & \dots & \cdot & \cdot & \cdot & \dots & \cdot \\ 0 & A_{N1}^{cc} & A_{N2}^{cc} & \dots & A_{NN}^{cc} & 0 & 0 & \dots & 0 \\ \hline 0 & 0 & 0 & \dots & 0 & A_{11}^{ss} & A_{12}^{ss} & \dots & A_{1N}^{ss} \\ 0 & 0 & 0 & \dots & 0 & A_{21}^{ss} & A_{22}^{ss} & \dots & A_{2N}^{ss} \\ \cdot & \cdot & \cdot & \dots & \cdot & \cdot & \cdot & \dots & \cdot \\ 0 & 0 & 0 & \dots & 0 & A_{N1}^{ss} & A_{N2}^{ss} & \dots & A_{NN}^{ss} \end{pmatrix}.$$



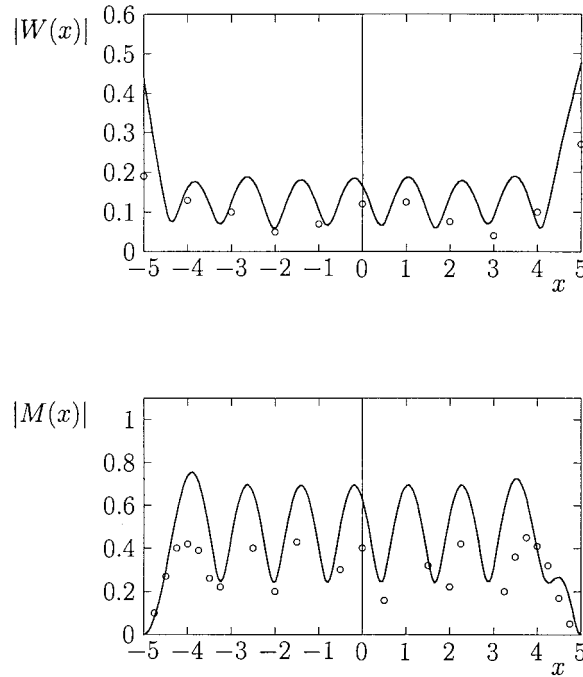


Figure 2. Amplitudes of the floating-plate deflection and bending moment.  $T = 0.7$ . Solid line – numerical results, circles – experimental data [9].

Matrix  $\mathbf{S}$  has the same form, which indicates that the even and odd parts of the hydroelastic problem for homogeneous beam can be separated and solved independently.

Numerical calculations were performed for the conditions of the experiments carried out by Wu *et al.* [9] for a homogeneous narrow plate in a channel. The experimental model was 10 m long, 50 cm wide and 38 mm thick, and had a density of  $220 \text{ kg/m}^3$ , an elastic modulus of 103 MPa and a draft of 8.36 mm. The experiment was performed at a water depth of 1.1 m, using incident wave heights of 5, 10 and 20 mm. In this case  $EJ = 471 \text{ kg m}^3/\text{s}^2$ ,  $L = 5 \text{ m}$ . The frequency of incident wave is equal to  $8.98 \text{ s}^{-1}$  (period of the wave  $T = 0.7 \text{ s}$ ),  $4.4 \text{ s}^{-1}$  (period of the wave  $T = 1.429 \text{ s}$ ) and  $2.2 \text{ s}^{-1}$  (period of the wave  $T = 2.875 \text{ s}$ ). As a result  $\beta = 7.7 \times 10^{-5}$ ,  $\alpha = 0.069$ ,  $\alpha = 0.016$  and  $\alpha = 0.004$ ,  $\gamma = 41.06$ ,  $\gamma = 9.85$  and  $\gamma = 2.43$ ,  $k = 41.06$ ,  $k = 10.1$  and  $k = 3.654$ , respectively, depending on the incident-wave frequency.

Convergence of the numerical algorithm was checked by changing the number of terms taken into account in each sum of expansions (20) and (21). It was found that the numerical results obtained with the number of retained terms greater than 50 are practically identical. Ninety terms ( $N = 90$ ) were used to plot the obtained numerical results.

The calculated amplitudes of both the beam deflection  $|W(x)|$  and the bending moments  $|M(x)|$  are shown in Figure 2 for  $T = 0.7 \text{ s}$ , in Figure 3 for  $T = 1.429 \text{ s}$  and in Figure 4 for  $T = 2.875 \text{ s}$  by solid lines. The results of the experiments by Wu *et al.* [9] are depicted by circles. It should be noted that agreement between the experimental and numerical results is fairly good.

The problem for a homogeneous beam was studied by Sturova [10] with the domain decomposition method, by Korobkin [8] with the normal mode method and by Wu *et al.* [9] with the help of a combination of these methods. The present results for the homogeneous beam are identical to those obtained in [8–10] by other methods. It should be noted that the numerical

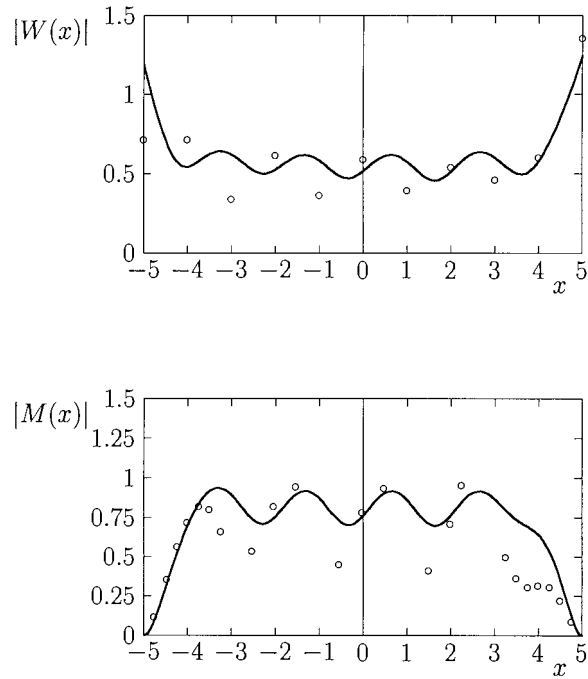


Figure 3. Amplitudes of the floating-plate deflection and bending moment.  $T = 1.429$ . Solid line – numerical results, circles – experimental data [9].

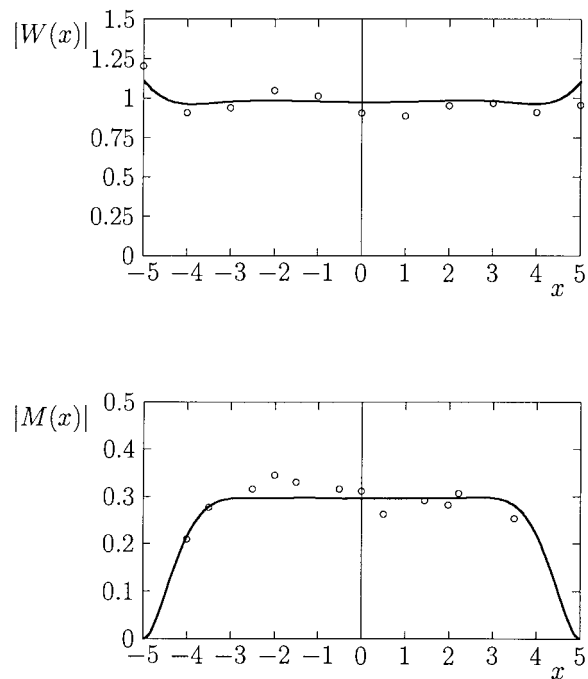


Figure 4. Amplitudes of the floating-plate deflection and bending moment.  $T = 2.875$ . Solid line – numerical results, circles – experimental data [9].

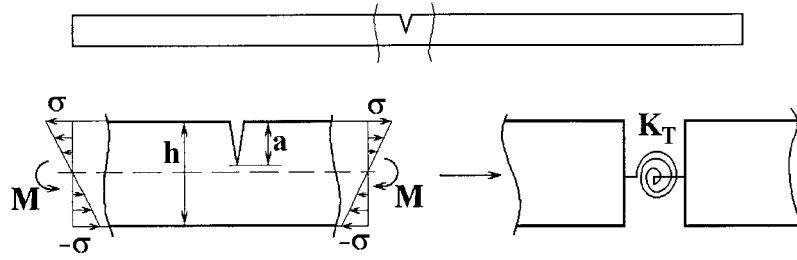
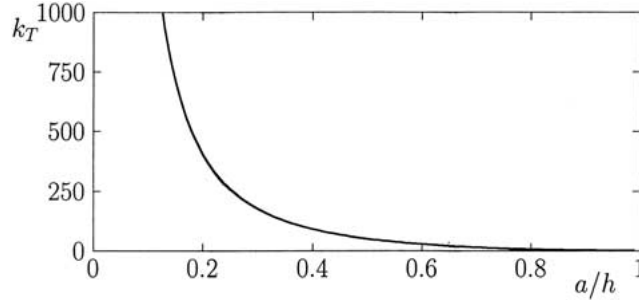


Figure 5. Scheme of the crack modeling.


 Figure 6. Torsional spring stiffness  $k_T$  as a function of  $a/h$ .

results from [8–10] are in good agreement for low frequencies of incident waves but differ from each other for high frequencies. The problem of high-frequency excitation of floating elastic plates has not yet been solved. The low-frequency case is considered here only.

## 5. Free-free cracked beam

Large floating structures of pontoon type are very flexible and may be damaged owing to periodic wave loads. In reality the structures initially contain small flaws (cracks, cavities and inclusions), which can absorb a part of the wave energy during fluid-structure interaction and can grow in time.

In the framework of the linear theory the presence of a crack is modeled with the help of a torsional spring (see Figure 5). The stiffness  $K_T$  of the equivalent torsional spring for a single-sided crack is assumed known as a function of the beam parameters and the crack length  $a$ . This function is presented in [11] and depicted in Figure 6. The solution for the floating free-free beam, which is divided into two parts by a torsional spring, provides the bending stresses outside the crack region. This solution together with the results by Bueckner [12] makes it possible to evaluate the stress distribution near the crack. This problem is not considered here.

The mathematical problem is described by Equations (14), (19) and conditions (15)–(17), where  $\alpha_1 = \alpha_2$ ,  $\beta_1 = \beta_2$ . The basic functions  $w_n^{(c)}(x)$ ,  $w_n^{(s)}(x)$  ( $n \geq 0$ ,  $m > 0$ ) will be given in Section 6 for more general case.

Calculations were performed for the conditions of the experiments by Wu *et al.* [9] with an homogeneous plate. Results of numerical calculations for two positions of the crack are presented in Figure 7 ( $l = -0.3$ ) and in Figure 8 ( $l = 0.15$ ). The results are depicted for an homogeneous beam ( $a = 0$ , curve 1) a broken beam ( $a = h$  curve 2) and a cracked beam ( $a/h = 0.8$  curve 3). Vibrations of the plate are generated by surface waves incident on the plate from the right.

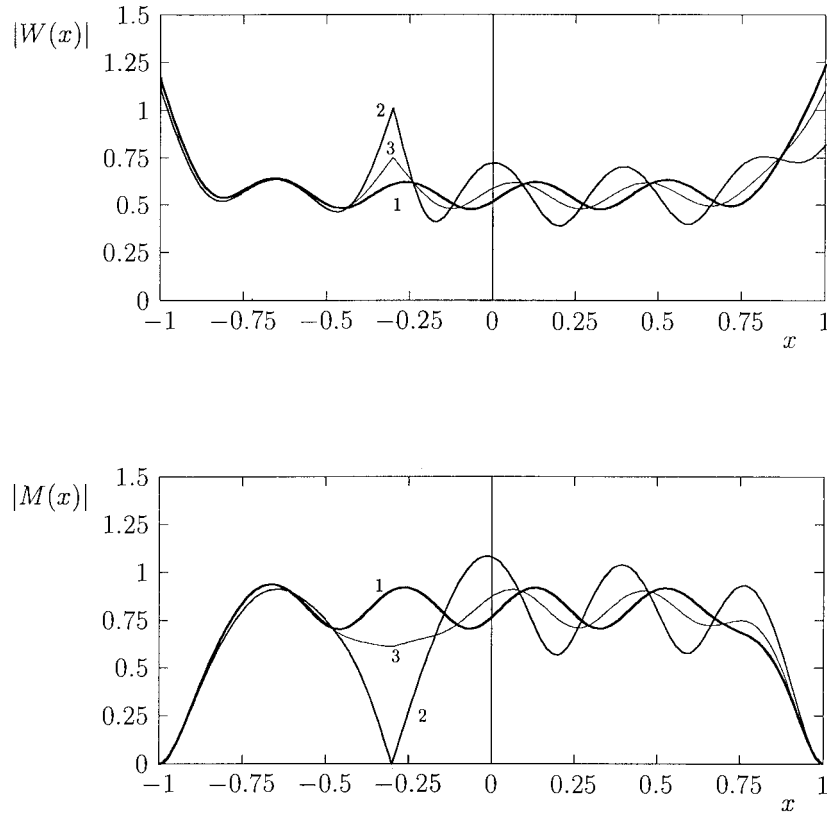


Figure 7. Amplitudes of the floating-plate deflection and bending moment.  $l = -0.3$ ,  $T = 1.429$ . Line 1 is for homogeneous beam ( $a = 0$ ), line 2 is for broken beam ( $a = h$ ) and line 3 is for cracked beam ( $a/h = 0.8$ ).

Analysis of numerical results obtained for different positions and lengths of the crack gives:

- Presence of a crack changes the distributions of both the plate deflections and stresses, provided the crack is longer than one half of the plate thickness. The longer the crack, the more pronounced are the changes.
- Local maximum of the deflections and local minimum of the bending stresses occur at the crack position.
- In front of the crack the stresses are greater and behind the crack they are smaller than for the homogeneous plate.
- These changes are more pronounced if the crack is located at the points of maximum bending stresses of the equivalent homogeneous plate.

## 6. Free-free compound beam

In order to model a floating plate with a vibration absorber, the linear problem of a compound beam is considered. The parts of the beam are connected with the help of a torsional spring. The longer part is referred to as the main structure, the characteristics of which are prescribed. The shorter part of the compound beam is referred to as an auxiliary plate, the length of which is given. Both characteristics of the auxiliary plate and the torsional spring stiffness, which essentially reduce the vibration amplitude of the main structure, must be determined. The

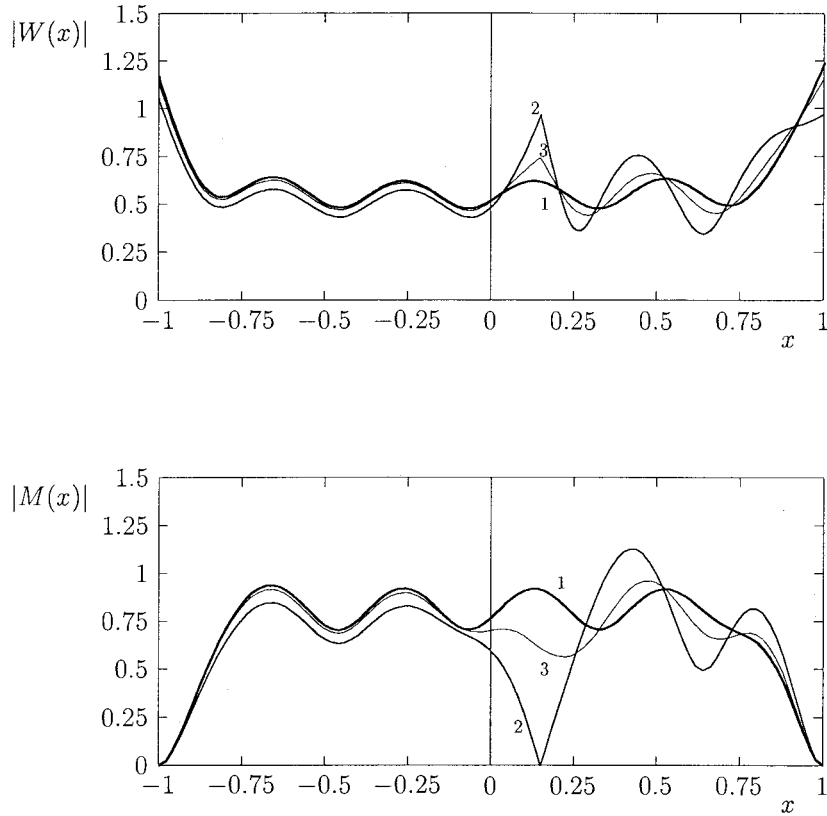


Figure 8. Amplitudes of the floating-plate deflection and bending moment.  $l = 0.15$ ,  $T = 1429$ . Line 1 is for homogeneous beam ( $a = 0$ ), line 2 is for broken beam ( $a = h$ ) and line 3 is for cracked beam ( $a/h = 0.8$ ).

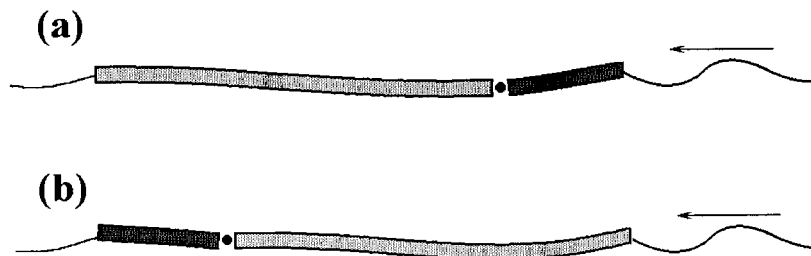


Figure 9. Floating structure with attached auxiliary plate: case  $a$  – in front of the main plate, case  $b$  – at the rear side of it.

auxiliary plate can be adjacent either in front of the structure (see Figure 9, case  $a$ ) or at the rear side of it (case  $b$ ).

The mathematical formulation of this problem is given by Equations (14), (19) with boundary conditions (15)–(17). In this case basic functions  $w_n^{(c)}(x)$ , ( $n \geq 0$ ) are determined as solutions of the problems

$$\beta(x) \frac{d^4 w_n^{(c)}}{dx^4} - \alpha(x) w_n^{(c)} = \cos(\pi n x) \quad (|x| < 1); \tag{30}$$

$$\frac{d^2 w_n^{(c)}}{dx^2}(\pm 1) = 0, \quad \frac{d^3 w_n^{(c)}}{dx^3}(\pm 1) = 0;$$

$$w_n^{(c)}(l-0) = w_n^{(c)}(l+0), \quad \beta_1 \frac{d^2 w_n^{(c)}}{dx^2}(l-0) = \beta_2 \frac{d^2 w_n^{(c)}}{dx^2}(l+0),$$

$$\beta_1 \frac{d^3 w_n^{(c)}}{dx^3}(l-0) = \beta_2 \frac{d^3 w_n^{(c)}}{dx^3}(l+0)$$

$$\frac{d^2 w_n^{(c)}}{dx^2}(l-0) + k_T \left[ \frac{dw_n^{(c)}}{dx}(l-0) - \frac{dw_n^{(c)}}{dx}(l+0) \right] = 0.$$

The functions  $w_n^{(c)}(x)$  can be presented as

$$w_n^{(c)}(x) = F_{1n} \cos \pi n x + D_{1n} \cos \lambda_1 x + D_{2n} \cosh \lambda_1 x + D_{3n} \sin \lambda_1 x + D_{4n} \sinh \lambda_1 x \\ (0 < x < l), \quad (31)$$

$$w_n^{(c)}(x) = F_{2n} \cos \pi n x + D_{5n} \cos \lambda_2 x + D_{6n} \cosh \lambda_2 x + D_{7n} \sin \lambda_2 x + D_{8n} \sinh \lambda_2 x \\ (0 < x < l), \quad (32)$$

where the coefficients  $D_{jn}$  ( $j = 1, 2, 3, \dots, 8$ ) are unknown in advance,  $\lambda_i = \sqrt[4]{\alpha_i/\beta_i}$  and  $F_{in} = 1/(\beta_i(\pi n)^4 - \alpha_i)$  ( $i = 1, 2$ ). Substitution of representations (31) and (32) in the boundary conditions leads to the linear algebraic system with respect to the coefficients  $D_{jn}$  (see Appendix). If we replace  $\cos \pi n x$  with  $\sin \pi n x$  in both Equation (30) and expressions (31), (32), we obtain the similar linear algebraic system for coefficients of the functions  $w_n^{(s)}(x)$  ( $n > 0$ ). Then using formulae (23)–(25) we can evaluate the elements of the matrix  $\mathbf{A}$ .

Calculations were performed for the conditions of experiments by Wu *et al.* [9] for the main plate. The period of the incident wave is equal to 1.429 s. Figure 10 shows the distribution of the beam deflection and the bending moment amplitudes, when the length of the auxiliary plate is equal to 1.5 m,  $(EJ)_{\text{aux}} = 10(EJ)_{\text{main}}$  and  $k_T = 0$ . Line 1 is for the single plate, line 2 for case (a) and line 3 for case (b). Figures 11 and 12 show the same quantities for the following parameters of the auxiliary plate:  $L_{\text{aux}} = 2.5$  m,  $(EJ)_{\text{aux}} = 100(EJ)_{\text{main}}$  with  $k_T = 0$  and  $k_T = 500$ , respectively.

The calculations were carried out for different values of the parameters of the auxiliary plate. It was revealed that:

- auxiliary plates adjacent in front of the main structure (case (a)) decrease the structure vibrations;
- vibrations of the main structure increase with auxiliary plates attached to its rear side (case (b));
- reduction of the vibrations is stronger if the plates are simply connected ( $k_T = 0$ );
- auxiliary plate of length 1.5 m decrease the deflections by 20% (case (a)) and increase them by 10% (case (b));
- essential reduction (35%) of the structure vibrations was obtained in the case of rigid auxiliary plates of length 2.5 m simply connected in front of the main structure.

Roughly speaking, in order to reduce the floating-plate vibrations, a rigid plate of smaller length has to be simply connected in front of the main structure.

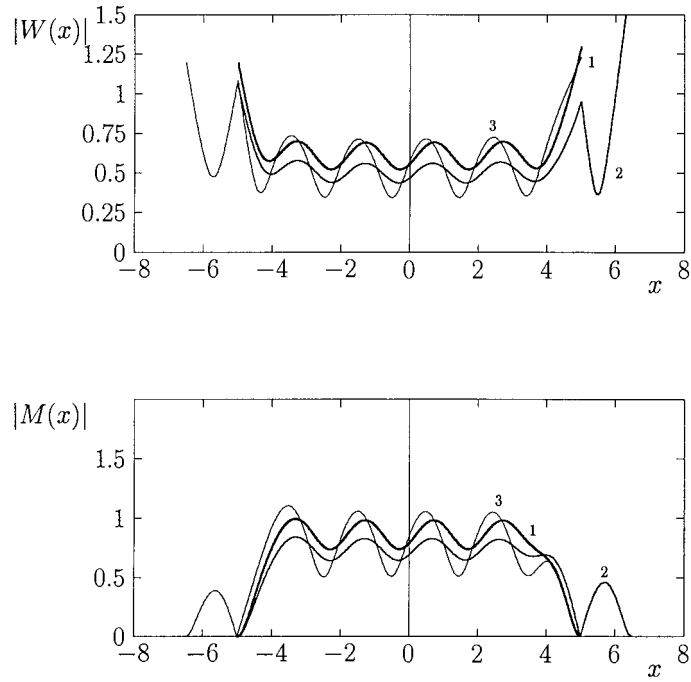


Figure 10. Amplitudes of the compound plate deflection and bending moment.  $T = 1.429$ ,  $L_{\text{aux}} = 0.15L_{\text{main}}$ ,  $(EJ)_{\text{aux}} = 10(EJ)_{\text{main}}$ ,  $k_T = 0$ . Line 1 is for a single plate, line 2 is for the case a, line 3 is for the case b.

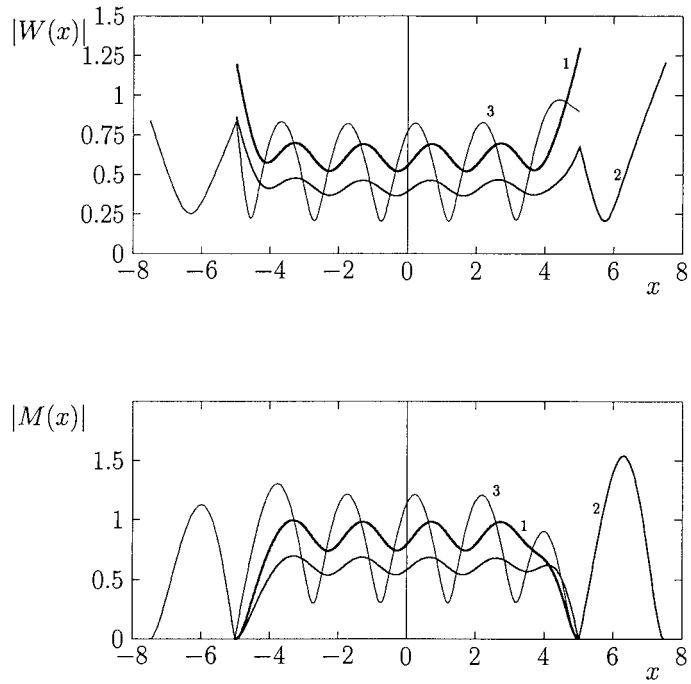


Figure 11. Amplitudes of the compound-plate deflection and bending moment.  $T = 1.429$ ,  $L_{\text{aux}} = 0.25L_{\text{main}}$ ,  $(EJ)_{\text{aux}} = 100(EJ)_{\text{main}}$ ,  $k_T = 0$ . Line 1 is for a single plate, line 2 is for the case a, line 3 is for the case b.

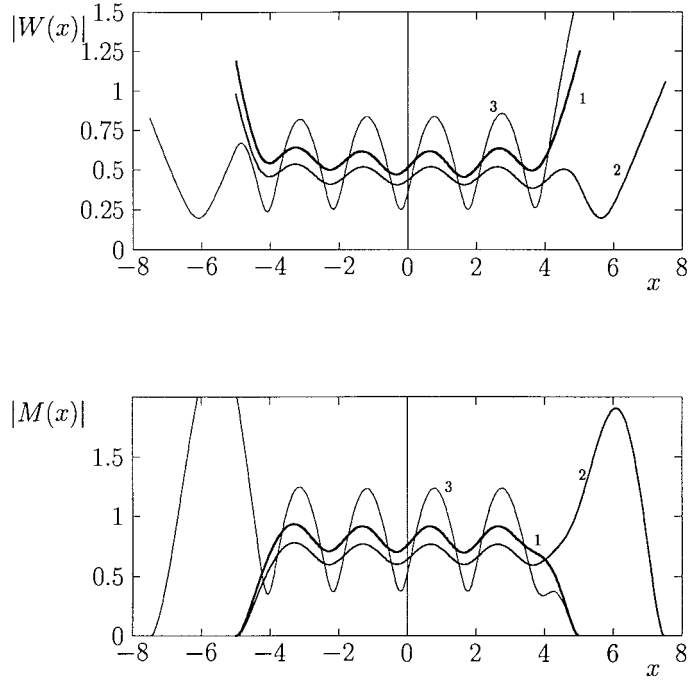


Figure 12. Amplitudes of the compound-plate deflection and bending moment.  $T = 1.429$ ,  $L_{\text{aux}} = 0.25L_{\text{main}}$ ,  $(EJ)_{\text{aux}} = 100(EJ)_{\text{main}}$ ,  $k_T = 500$ . Line 1 is for a single plate, line 2 is for the case a, line 3 is for the case b.

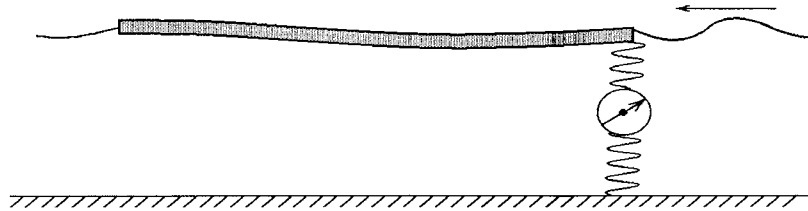


Figure 13. Fluid-structure system with plate edge being elastically connected to the sea bottom.

### 7. Floating beam with its edge being elastically connected to the sea bottom

The solution of problem (19)–(20) with  $\alpha_1 = \alpha_2$ ,  $\beta_1 = \beta_2$ ,  $k_T = \infty$  and boundary conditions

$$W''(\pm 1) = 0, \quad W'''(-1) = 0, \quad W'''(+1) = -k_l W(+1)$$

describes the hydroelastic behaviour of an homogeneous floating beam with its edge being elastically connected to the sea bottom (see Figure 13). Here  $k_l = K_l L^3 / EJ$ , where  $K_l$  is the stiffness of the connecting spring. It was revealed that elastic connection of the front edge to the bottom can essentially reduce the beam deflections in the main part of the beam. Rigidity of the elastic connector can be selected in an optimal way for a given frequency of incident wave.

In this case the basic functions  $w_n^{(c)}(x)$ , ( $n \geq 0$ ) are determined as solutions of the problems

$$\beta \frac{d^4 w_n^{(c)}}{dx^4} - \alpha w_n^{(c)} = \cos(\pi n x) \quad (|x| < 1); \tag{33}$$

$$\frac{d^2 w_n^{(c)}}{dx^2}(\pm 1) = 0, \quad \frac{d^3 w_n^{(c)}}{dx^3}(-1) = 0, \quad \frac{d^3 w_n^{(c)}}{dx^3}(1) = -k_l w_n^{(c)}; \tag{34}$$



and are sought in the forms

$$w_n^{(c)}(x) = F_n \cos \pi n x + D_{1n} \cos \lambda x + D_{2n} \cosh \lambda x + D_{3n} \sin \lambda x + D_{4n} \sinh \lambda x. \quad (35)$$

Here  $D_{jn}$  ( $j = 1, 2, 3, 4$ ) are unknown coefficients,  $\lambda = \sqrt[4]{\alpha/\beta}$  and  $F_n = 1/(\beta(\pi n)^4 - \alpha)$ . As in the previous cases, we substitute (35) in the boundary conditions (34), which leads to a linear algebraic system with respect to the unknown coefficients:

$$\mathbf{T} \vec{D}_n = \vec{F}_n,$$

where

$$\vec{F}_n = ((-1)^n (\pi n)^2 F_n, 0, (-1)^n (\pi n)^2 F_n, -k_l F_n)^T, \quad \vec{D}_n = (D_{1n}, D_{2n}, D_{3n}, D_{4n})^T$$

and the matrix  $\mathbf{T}$  has the form

$$\mathbf{T} = \begin{pmatrix} -\lambda^2 \cos \lambda & \lambda^2 \cosh \lambda & \lambda^2 \sin \lambda & -\lambda^2 \sinh \lambda \\ -\lambda^3 \sin \lambda & -\lambda^3 \sinh \lambda & -\lambda^3 \cos \lambda & \lambda^3 \cosh \lambda \\ -\lambda^2 \cos \lambda & \lambda^2 \cosh \lambda & -\lambda^2 \sin \lambda & \lambda^2 \sinh \lambda \\ \lambda^3 \sin \lambda + k_l \cos \lambda & \lambda^3 \sinh \lambda + k_l \cosh \lambda & -\lambda^3 \cos \lambda + k_l \sin \lambda & \lambda^3 \cosh \lambda + k_l \sinh \lambda \end{pmatrix}.$$

If we replace  $\cos \pi n x$  by  $\sin \pi n x$  in Equations (33) and (35), we obtain a similar algebraic system for the coefficients of the functions  $w_n^{(s)}(x)$  ( $n > 0$ ). Matrix  $\mathbf{T}$  of this system is the same, but the vector  $F_n$  has the form

$$\vec{F}_n = (0, (-1)^n (\pi n)^3 F_n, 0, (-1)^n (\pi n)^3 F_n - k_l F_n)^T.$$

After the functions  $w_n^{(c)}(x)$  and  $w_n^{(s)}(x)$  have been found, the matrix  $\mathbf{A}$  is obtained in the same manner as before.

Figure 14 shows the amplitudes of the beam deflections and the bending moments for the free-free beam ( $k_l = 0$ , curve 1) and for an elastically connected beam ( $k_l = 770$  curve 2;  $k_l = 1000$  solid curve 3 and  $k_l = 600$  dotted curve 3). The parameters of the numerical calculations are the same as in experiments by Wu *et al.* [9] with the wave period  $T = 1.429$  s. One can see the curve with  $k_l = 1000$  is similar to the curve with  $k_l = 600$ . It is seen that the dimensional rigidity of the elastic connector  $k_l = 770$ , which corresponds to  $K_l \approx 2930$  kg/s<sup>2</sup>, can be considered as optimal for the experimental conditions [9]. For another frequency of the incident wave the connector rigidity has to be changed, which can be done with an active control system.

## 8. Conclusion

In this paper several two-dimensional problems of floating-plate behaviour in waves were analyzed. These problems are: free-free homogeneous beam in waves, cracked beam in waves, compound beam with an elastic connection between its parts and homogeneous floating beam which is elastically connected to the sea bottom. All problems are treated by a common method. This method is based on hydroelasticity, in which the coupled hydrodynamics and structural-dynamics problems are solved simultaneously. Deflections and bending moments in the plate, as well as approaches for their reduction, have been analyzed using the developed method.

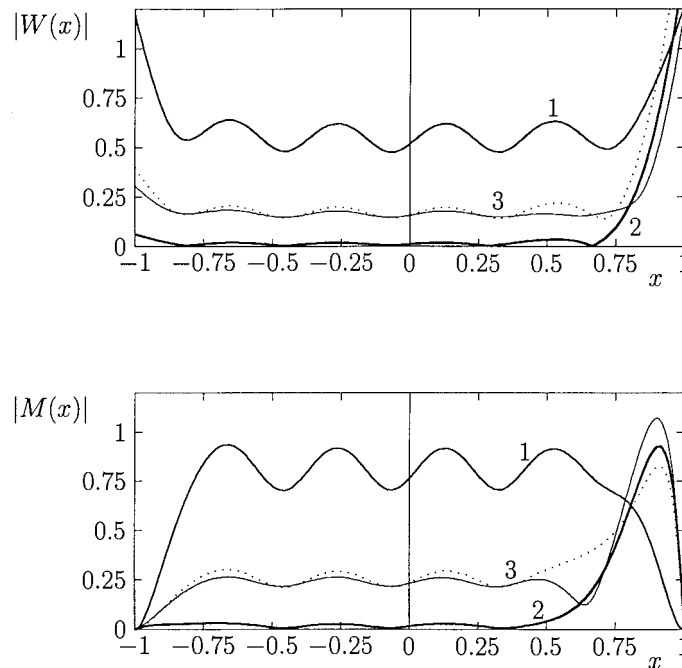


Figure 14. Amplitudes of the moored plate deflection and bending moment.  $T = 1.429$ . Line 1 is for the free-free beam ( $k_l = 0$ ), line 2 is for elastically connected beam ( $k_l = 770$ ), solid line 3 is for  $k_l = 1000$  and dotted line 3 is for  $k_l = 600$ .

A main idea of the presented method is to use different basic functions for the pressure distribution and the beam deflection. Trigonometric functions are used as basic functions for the hydrodynamic part of the problem. The elastic part of the coupled problem in each particular case was reduced to a boundary-value problem for a simple pressure distribution: either  $\cos \pi n x$  or  $\sin \pi n x$ . As a result, the treatment of the hydrodynamic part of the problem was simplified and at the same time the beam boundary conditions were accurately satisfied.

With the help of the developed method two approaches aimed to reduce the plate vibration were studied. It was shown that, in order to reduce the floating-plate vibrations, a rigid plate of smaller length has to be simply connected in front of the main structure. In the second approach the floating beam is connected to the sea bottom with a spring. It was demonstrated that the spring rigidity can be selected in an optimal way for a given frequency of the incident wave, in order to reduce the deflections of the main part of the plate. In both cases the effect of the vibration reduction is quite pronounced and can be utilized at the design stage.

The developed method can be used to treat other hydroelastic problems of very large floating structures with different boundary conditions at the plate edges and different design features.

### Acknowledgements

This work was supported by the Russian Fund of Basic Research (projects N00-01-00842, N00-01-00850 and N00-15-96162), by Integration grant NI of the Siberian Branch RAS and by grant N97 (6-1999) of the RAS for young scientists.

**Appendix**

To find the undetermined coefficients  $D_{in}$  ( $j = 1, 2, 3, \dots, 8$ ) we have the linear algebraic system:

$$\begin{aligned}
 & -\lambda_1^2 \cos \lambda_1 D_{1n} + \lambda_1^2 \cosh \lambda_1 D_{2n} + \lambda_1^2 \sin \lambda_1 D_{3n} - \lambda_1^2 \sinh \lambda_1 D_{4n} = (-1)^n (\pi n)^2 F_{1n}, \\
 & -\lambda_1^3 \sin \lambda_1 D_{1n} - \lambda_1^3 \sinh \lambda_1 D_{2n} - \lambda_1^3 \cos \lambda_1 D_{3n} + \lambda_1^3 \cosh \lambda_1 D_{4n} = 0, \\
 & -\lambda_2^2 \cos \lambda_2 D_{5n} + \lambda_2^2 \cosh \lambda_2 D_{6n} - \lambda_2^2 \sin \lambda_2 D_{7n} + \lambda_2^2 \sinh \lambda_2 D_{8n} = (-1)^n (\pi n)^2 F_{2n}, \\
 & \lambda_2^3 \sin \lambda_2 D_{5n} + \lambda_2^3 \sinh \lambda_2 D_{6n} - \lambda_2^3 \cos \lambda_2 D_{7n} + \lambda_2^3 \cosh \lambda_2 D_{8n} = 0, \\
 & \cos \lambda_1 l D_{1n} + \cosh \lambda_1 l D_{2n} + \sin \lambda_1 l D_{3n} + \sinh \lambda_1 l D_{4n} - \cos \lambda_2 l D_{5n} - \cosh \lambda_2 l D_{6n} - \\
 & - \sin \lambda_2 l D_{7n} - \sinh \lambda_2 l D_{8n} = (F_{1n} - F_{2n}) \cos \pi n l, \\
 & -\lambda_1^2 \cos \lambda_1 l D_{1n} + \lambda_1^2 \cosh \lambda_1 l D_{2n} - \lambda_1^2 \sin \lambda_1 l D_{3n} + \lambda_1^2 \sinh \lambda_1 l D_{4n} + \quad (A.1) \\
 & + \lambda_2^2 \delta \cos \lambda_2 l D_{5n} - \lambda_2^2 \delta \cosh \lambda_2 l D_{6n} + \lambda_2^2 \delta \sin \lambda_2 l D_{7n} - \lambda_2^2 \delta \sinh \lambda_2 l D_{8n} \\
 & = (F_{1n} - \delta F_{2n}) (\pi n)^2 \cos \pi n l, \\
 & \lambda_1^3 \sin \lambda_1 l D_{1n} + \lambda_1^3 \sinh \lambda_1 l D_{2n} - \lambda_1^3 \cos \lambda_1 l D_{3n} + \lambda_1^3 \cosh \lambda_1 l D_{4n} - \\
 & - \lambda_2^3 \delta \sin \lambda_2 l D_{5n} - \lambda_2^3 \delta \sinh \lambda_2 l D_{6n} + \lambda_2^3 \delta \cos \lambda_2 l D_{7n} - \lambda_2^3 \delta \cosh \lambda_2 l D_{8n} \\
 & = -(F_{1n} - \delta F_{2n}) (\pi n)^3 \sin \pi n l, \\
 & (-\lambda_1^2 \cos \lambda_1 l - k_T \lambda_1 \sin \lambda_1 l) D_{1n} + (\lambda_1^2 \cosh \lambda_1 l + k_T \lambda_1 \sinh \lambda_1 l) D_{2n} + \\
 & (-\lambda_1^2 \sin \lambda_1 l + k_T \lambda_1 \cos \lambda_1 l) D_{3n} + (\lambda_1^2 \sinh \lambda_1 l + k_T \lambda_1 \cosh \lambda_1 l) D_{4n} \\
 & + k_T \lambda_2 \sin \lambda_2 l D_{5n} - \\
 & - k_T \lambda_2 \sinh \lambda_2 l D_{6n} - k_T \lambda_2 \cos \lambda_2 l D_{7n} - k_T \lambda_2 \cosh \lambda_2 l D_{8n} = F_{1n} (\pi n)^2 \cos \pi n l \\
 & + (F_{1n} - F_{2n}) k_T (\pi n) \sin \pi n l.
 \end{aligned}$$

Here  $\delta = \beta_1 / \beta_2$ .

The functions  $w_n^{(s)}(x)$  ( $n > 0$ ) have the forms

$$\begin{aligned}
 w_n^{(s)}(x) &= F_{1n} \sin \pi n x + D_{1n} \cos \lambda_1 x + D_{2n} \cosh \lambda_1 x + D_{3n} \sin \lambda_1 x + D_{4n} \sinh \lambda_1 x, \\
 & (0 < x < l),
 \end{aligned}$$

$$\begin{aligned}
 w_n^{(s)}(x) &= F_{2n} \sin \pi n x + D_{5n} \cos \lambda_2 x + D_{6n} \cosh \lambda_2 x + D_{7n} \sin \lambda_2 x + D_{8n} \sinh \lambda_2 x, \\
 & (l < x < 1),
 \end{aligned}$$

The coefficients  $D_{in}$  ( $j = 1, 2, 3, \dots, 8$ ) satisfy system (A.1) with its right-hand side being replaced now by the vector

$$(0, (-1)^n(\pi n)3F_{1n}, 0, (-1)^n(\pi n)3F_{2n}, (F_{1n} - F_{2n}) \sin \pi nl, (F_{1n} - \delta F_{2n})(\pi n)^2 \sin \pi nl, \\ (F_{1n} - \delta F_{2n})(\pi n)^3 \cos \pi nl, F_{1n}(\pi n)^2 \sin \pi nl - (F_{1n} - F_{2n})k_T(\pi n) \cos \pi nl)^T.$$

## References

1. H. Suzuki, K. Yoshida, Design flow and strategy for safety and very large floating structure. In: Watanabe (ed.), *Proc. Int. Workshop on Very Large Floating Structures* (1996) pp. 21–27.
2. S. Nagata, H. Yoshida, T. Fujita, H. Isshiki, Reduction of the motion of and elastic floating plate in waves by breakwaters. In: M. Kashiwagi, W. Koterayama and M. Ohkusu (eds.), *Proc. 2 Int. Conf. on Hydroelasticity in Marine Technology*, Fukuoka, Japan, 1-3 Dec. (1998) pp. 229–238.
3. H. Seto, M. Ochi, A hybrid element approach to hydroelastic behavior of a very large floating structure in regular wave. *Proc. 2 Int. Conf. on Hydroelasticity in Marine Technology*, Fukuoka, Japan, 1-3 Dec. (1998) pp. 185–194.
4. K. Yago, H. Endo, S. Ohmatsu, On the hydroelastic response of box-shaped floating structure with shallow draft (2nd report). *J. Soc. Nav. Arch. Japan*. 182 (1997) 307–817.
5. M. Kashiwaga, Hydrodynamic interactions among a great number of columns supporting a very large flexible structure. In: M. Kashiwagi, W. Koterayama and M. Ohkusu (eds.), *Proc. 2 Int. Conf. on Hydroelasticity in Marine Technology*, Fukuoka, Japan, 1-3 Decem (1998) pp. 165–176.
6. J.W. Kim, R.C. Ertekin, An eigenfunction-expansion method for predicting hydroelastic behavior of a shallow-draft VLFS. *Proc. 2 Int. Conf. on Hydroelasticity in Marine Technology*, Fukuoka, Japan, 1-3 Dec. (1998) pp. 47–60.
7. A.A. Shabana, *Theory of Vibration (An Introduction)*, (2nd ed.). Mechanical Engineering Series. Berlin: Springer (1996) 347 pp.
8. A.A. Korobkin, Numerical and asymptotic study of the two-dimensional problem on hydroelastic behavior of a floating plate in waves. *J. Appl. Mech. Tech. Phys.* 41 (2000) 286–293.
9. C. Wu, E. Watanabe and T. Utsunomiya, An eigenfunction expansion-matching method for analyzing the wave-induced responses of an elastic floating plate. *Appl. Ocean Res.* 17 (1995) 301–310.
10. I.V. Sturova, The oblique incidence of surface waves onto the elastic band. In: M. Kashiwagi, W. Koterayama and M. Ohkusu (eds.), *Proc. 2nd Int. Conf. on Hydroelasticity in Marina Technology*, Fukuoka, Japan, 1-3 Dec. (1998) pp. 239–245.
11. P.F. Rizos, N. Aspragathos, Dimarogonas, Identification of crack location and magnitude in a cantilever beam from the vibration modes. *J. Sound Vib.* 138 (1990) 381–388.
12. H.F. Bueckner, Some stress singularities and their computation by means of integral equations. In: R.E. Langer (ed.), *Proceedings of Symposium Boundary Problems in Differential Equations*, 20-22 April 1959. Madison: U. Wisconsin Press (1960) pp. 215–230.